HUMAN MUTATION 28(4), 356–364, 2007

RESEARCH ARTICLE

Truncation of *NHEJ1* in a Patient With Polymicrogyria

Vincent Cantagrel,[1,2] Anne-Marie Lossi,[1,2] Steven Lisgo,[3] Chantal Missirian,[1,4] Ana Borges,[1,2] Nicole Philip,[1,4] Carla Fernandez,[5] Carlos Cardoso,[1,2] Dominique Figarella-Branger,[5] Anne Moncla,[1,4] Susan Lindsay,[3] William B. Dobyns,[6–8] and Laurent Villard[1,2]*

[1]*INSERM, U491, Faculté de Médecine La Timone, Marseille, France;* [2]*Aix Marseille Université, Faculté de Médecine, Marseille, France;* [3]*Institute of Human Genetics, International Centre for Life, Newcastle, United Kingdom;* [4]*Department of Medical Genetics, La Timone Children's Hospital, Marseille, France;* [5]*Nervous et Muscular Biopathology, Faculté de Médecine La Timone, Marseille, France;* [6]*Department of Human Genetics, The University of Chicago, Chicago, Illinois;* [7]*Department of Neurology, The University of Chicago, Chicago, Illinois;* [8]*Department of Pediatrics, The University of Chicago, Chicago, Illinois*

Communicated by Maria Rita Passos-Bueno

Polymicrogyria (PMG) is a common malformation of the human cerebral cortex for which both acquired and genetic causes are known. Although genetic heterogeneity is documented, only one gene is currently known to cause isolated PMG. To clone new genes involved in this type of cerebral malformation, we studied a fetus presenting a defect of cortical organization consisting of a polymicrogyric cortex and neuronal heterotopia within the white matter. Karyotype analysis revealed that the fetus was carrier of a balanced, de novo, chromosomal translocation t(2;7)(q35;p22). Cloning and sequencing of the two translocation breakpoints reveals that the chromosomal rearrangement disrupts the coding region of a single gene, called *NHEJ1*, *Cernunnos*, or *XLF*, in 2q35. The *NHEJ1* gene was recently identified as being responsible for autosomal recessive immunodeficiency with microcephaly. Using quantitative PCR experiments, we show that a truncated transcript is expressed in the polymicrogyric patient cells, suggesting a potential dominant negative effect possibly leading to a different phenotype. We performed in situ hybridization on human embryos and showed that the *NHEJ1* transcript is preferentially expressed in the telencephalic ventricular and subventricular zones, consistent with the phenotype of the affected individual. In the human adult central nervous system (CNS), *NHEJ1* is mainly expressed in the cerebral cortex and in the cerebellum. The association of PMG with the disruption of its transcript suggests that, in addition to its recently uncovered function in the immune system, the NHEJ1 protein may also play a role during development of the human cerebral cortex. Hum Mutat 28(4), 356–364, 2007. **© 2006 Wiley-Liss, Inc.**

KEY WORDS: polymicrogyria; human embryo; XLF; Cernunnos; NHEJ1; cortical dysplasia

INTRODUCTION

Malformations of cortical development, also called cortical dysplasia, are a common cause of epilepsy and cognitive deficits. Recent estimates have suggested that up to 25% of adults and 40% of children with intractable epilepsy have cortical dysplasia [Kuzniecky and Jackson, 1995; Meencke and Veith, 1992; Vinters et al., 1992]. Polymicrogyria (PMG) is a well-known and relatively common malformation of cortical development that consists of an irregular brain surface, loss of the normal gyral pattern, which is replaced by many small and infolded gyri separated by shallow sulci that are often partly fused in their depths, and reduction of the normal six-layered cortex to a four-layered or unlayered cortex. Affected individuals present with variable phenotypes that range from severe neonatal encephalopathies to normal intelligence with specific cognitive defects, depending on the extent and specific location of PMG, as well as overall head size, although most patients have mental retardation [Guerrini et al., 2003]. Seizures typically begin between 4 and 12 years of age and are often intractable.

Despite many descriptions, the pathogenesis of PMG remains poorly understood, and is likely to be heterogeneous. Older reports support extrinsic causes, especially vascular causes such as intrauterine cytomegalovirus infection and placental perfusion problems as may occur with twinning, and point to a period of risk between 13 and 24 weeks gestation [Barkovich and Lindan, 1994; Barth, 1992; Iannetti et al., 1998]. Substantial other evidence supports a genetic basis for PMG including reports of familial recurrence consistent with autosomal or X-linked inheritance

Received 11 July 2006; accepted revised manuscript 17 October 2006.

*Correspondence to: Laurent Villard, INSERM U491, Faculté de Médecine de La Timone, 27 Bd. Jean Moulin, 13385 Marseille Cedex 5, France. E-mail: laurent.villard@medecine.univ-mrs.fr

Grant sponsor: INSERM; Grant sponsor: Programme Hospitalier de Recherche Clinique (PHRC National 2004); Grant sponsor: le Groupement d'Intérêt Scientifique (GIS) Institut des Maladies Rares.

DOI 10.1002/humu.20450

Published online 26 December 2006 in Wiley InterScience (www.interscience.wiley.com).

[reviewed in Jansen and Andermann, 2005], our report of a PMG locus in Xq28 [Villard et al., 2002], and association with several chromosome abnormalities, particularly involving the DiGeorge syndrome critical region in chromosome 22q11.2 [Robin et al., 2006]. PMG has also been reported in several multiple congenital anomaly syndromes, such as Adams-Oliver (MIM# 100300), Aicardi (MIM# 304050), Goldberg-Shprintzen (MIM# 182212), (Warburg) Micro (MIM# 600118), and oculocerebrocutaneous (Delleman) (MIM# 164180) syndromes. However, mutations of only a few genes have been associated with PMG. The first is RAB3GAP, which regulates the Rab3 pathway implicated in exocytic release of neurotransmitters, hormones, and possibly trophic factors, and is mutated in some patients with Micro syndrome [Aligianis et al., 2005]. The next is KIAA1279, a gene of unknown function that is mutated in Goldberg-Shprintzen syndrome [Brooks et al., 2005]. Finally, both heterozygous and especially homozygous mutations of PAX6 have been associated with PMG [Glaser et al., 1994; Mitchell et al., 2003].

In addition, several atypical cortical malformations that grossly resemble PMG but differ on detailed review have been described in neonatal adrenoleukodystrophy and Zellweger syndrome [Evrard et al., 1978; Kelley et al., 1986], the cobblestone cortical malformations found in Fukuyama congenital muscular dystrophy, muscle-eye-brain and Walker-Warburg syndromes [Dobyns et al., 1989; Haltia et al., 1997; Takada et al., 1988], and cobblestone-like changes associated with mutations of the GPR56 and SNAP29 genes [Chang et al., 2003; Piao et al., 2004, 2005; Sprecher et al., 2005].

In our experience, informative families useful for mapping Mendelian forms of typical PMG are rare. An alternative strategy to identify disease genes is to take advantage of de novo chromosomal rearrangements in affected patients. This strategy has led to the identification of a large number of genes, including genes implicated in different types of cortical dysplasia such as lissencephaly either due to *LIS1* [Lo Nigro et al., 1997] or *DCX* mutations [Gleeson et al., 1998], or periventricular nodular heterotopia due to *FLNA* mutations [Fox et al., 1998].

We studied a fetus with a brain malformation consisting of diffuse PMG and small mostly submicroscopic heterotopia distributed throughout the white matter. Chromosome analysis demonstrated an apparently balanced, chromosomal translocation: 46,XX, t(2;7)(q35;p22) de novo. We showed that the rearrangement is molecularly balanced and that it disrupts the coding region of the *NHEJ1* (also called *Cernunnos*, *XLF*, or *FLJ12610*) gene in 2q35. *NHEJ1* encodes a very recently described 33-kDa protein that is a component of the mammalian DNA nonhomologous end-joining (NHEJ) apparatus [Ahnesorg et al., 2006; Buck et al., 2006]. The NHEJ1 protein interacts with XRCC4 and promotes the repair of double strand breaks in mammalian cells [Callebaut et al., 2006]. Mutations in this gene are found in patients affected by an autosomal recessive form of immunodeficiency with microcephaly. The expression of this gene during development has not been previously described. We performed in situ hybridization on human embryos and show that the *NHEJ1* transcript is preferentially expressed in the telencephalic ventricular and subventricular zones, consistent with the phenotype of the affected individual. We also show that a truncated transcript is expressed in the patient's cells. Because NHEJ1 needs to form homo- and heterodimers to function properly, we discuss the possibility that the phenotype of our patient is the result of a dominant negative effect. The association of PMG with the disruption of this transcript suggests that, in addition to its recently uncovered function in the immune system, the *NHEJ1* gene may also play a role during development of the human cerebral cortex.

MATERIALS AND METHODS

Fluorescent In Situ Hybridization (FISH) on Metaphase Chromosomes

BAC DNA prepared according to standard procedures was labeled by nick translation. The reactions were carried out in a volume of 50 mL with 1 mg of DNA, 50 μM Tris Hcl, 5 mM $MgCl_2$, 10 mM β-mercaptoethanol, 10 μg/mL bovine serum albumin (BSA), 50 μM dATP, dCTP and dGTP, 30 μM of dTTP, 20 μM of dUTP labeled with Spectrum Green or Spectrum Orange (Vysis, Downers Grove, IL; www.vysis.com), and 2.5 U of DNA polymerase I/Dnase I mix (Invitrogen, Carlsbad, CA; www.invitrogen.com). The reactions were incubated at 15°C for 45 minutes and 16 μg of human Cot1 DNA and 800 μg of salmon sperm DNA were added before ethanol precipitation. The dry pellets were resuspended with the hybridization buffer (formamide 50%, 2 × salt saline citrate (SSC), SDS 10%, sulfate dextran 10%, Denhardt's buffer 1 ×, pH 7). Hybridization was performed as previously described [Chong et al., 1997]. Chromosomes were counterstained with 4′,6′-diamino-2-phenylindole (DAPI) and observed using a Zeiss Axiophot microscope. Images were collected using a charge-coupled device (CCD) camera (Sensys-Photometrics, Tucson, AZ; www.photomet.com/support_sensys.html) and Quips Lab manager (Vysis).

Cell Culture, RNA Isolation, and Reverse Transcription

All lymphoblastoid cell lines were grown in RPMI 1680 (Invitrogen) with 10% fetal bovine serum in the presence of 0.1 mg/ml of kanamycin at 37°C and 5% CO_2. Total RNA was extracted from patient's cells using TRIzol reagent (Invitrogen). The RNA preparations were analyzed for purity using the ND-1000 spectrophotometer (NanoDrop, Wilmington, DE; www.nanodrop.com). DNAse treatment was performed for 30 minutes with 5 μg of RNA, 5U of RNAse-free DNAse I (Roche, Basel, Switzerland; www.roche-diagnostics.com/researchers/molecularbiology.html). Human normal tissue RNA was purchased (BD Biosciences, San Jose, CA; www.bdbiosciences.com). Reverse transcription of 5 μg of total RNA was performed in 50 μl of 1 × Superscript reaction buffer (Invitrogen) containing 3 ng/μl of dN6, 40U of RNasin (Promega, Madison, WI; www.promega.com/), 10 mM dNTP, and 200 U of Superscript II reverse transcriptase (Invitrogen). For every reaction, one RNA sample was treated similarly without Superscript II RT (RT-reaction) to provide a negative control.

Northern and Southern Blot Hybridizations

We hybridized human fetal MTN blot II and human brain MTN blot II (BD Biosciences) with a *NHEJ1* cDNA probe (nucleotides 78–1061 of the cDNA sequence BC030986) and a probe for β-actin (BD Bioscience,). These probes were labeled by random priming using [α-^{32}P]dCTP. Hybridization of Northern blots were carried out in 50% formamide buffer at 42°C for 16 hr. For Southern blot preparation, DNA samples were digested with *HpaI*, electrophoresed on 1% agarose gel, and blotted onto Hybond N+ nylon membrane (GE Healthcare, Chalfont St-Giles, UK; www.gehealthcare.com). Hybridization and washing were carried out, respectively, in 5 × SSC/0.5% SDS/ 1 × Denhardt's buffer, and 0.1 × SSC/0.1% SDS at 65°C according to standard procedures.

Classical and Real-Time PCR

Classical PCR reactions were performed in the T1 thermocycler (Whatman-Biometra, Goettingen, Germany; www.biometra.de) in

a total volume of 50 µl, containing 1 × PCR buffer, 0.2 mM dNTPs, 2 mM $MgCl_2$, and 1U Taq polymerase (Invitrogen).

Real-time PCR reactions were performed in the LightCycler 480 system (Roche) using the SYBR Green I Master Kit (Roche) with 1 µL cDNA (1/5 dilution of the first strand reaction), 100 to 300 nM of each primer. Each reaction was performed in duplicate. The results were imported and analyzed using Excel (Microsoft Corporation, Redmond, WA; www.microsoft.com).

Mutation Screening

A total of 85 patients with PMG were investigated: 10 patients with PMG and periventricular nodular heterotopia, three patients with PMG and subcortical nodular heterotopia, and 72 patients with bilateral perisylvian PMG. In each case, DNA from affected individuals was used for direct sequencing of *NHEJ1*. We designed primer pairs for each of the seven coding exons including exon–intron boundary sequences. We used the following primers: exon 2 (459-bp product) forward (5′-GGAGAACGTA AATCCATGCC-3′) and reverse (3′-CCTGTACTTCTGCCTGG AAT-5′); exon 3 (389-bp product) forward (5′-TCTCATGTCCA TTGCCTTCG-3′) and reverse (3′-GAGAGGAAGCTTTAGGT GCT-5′); exon 4 (299-bp product) forward (5′-CTGGTACC TAATACTGAATTGG-3′) and reverse (3′-GGGAGACTCATT TGCATTAGA-5′); exon 5 (358-bp product) forward (5′-ACTGA ACTAGGTGTCTCTGC-3′) and reverse (3′-GGCTTGAGATG TACTTAGGG-5′); exon 6 (328-bp product) forward (5′-CCAGG CTTGGATATGGTCG-3′) and reverse (3′-GGATCTAGGTTTA TGCTGTCC-5′); exon 7 (294-bp product) forward (5′-ATCAGA ATGCTTGGTGAATGC-3′) and reverse (3′-GGAATTGCTGCT TCATTGG-5′); exon 8 (377-bp product) forward (5′-CTCATCC TAACCAGGAGCC-3′) and reverse (3′-GGAAGCCAGTCTCT GAGAAT-5′). We sequenced all exons in both forward and reverse directions. Sequencing was carried out by GATC Biotech (Constance, Germany; www.gatc-biotech.com/en/index.php) and Sequencer software (Gene Codes, Ann Arbor, MI; www.genecodes.com) was used to analyze sequences and chromatograms.

Electronic Database Information

GenBank accession numbers for BAC clones are as follows: AC068946 (RP11-803J6) and AC073316 (RP11-191P7). Genomic clones were obtained from the Sanger Centre (Cambridgeshire, England, UK; now called the Wellcome Trust Sanger Institute). BAC contigs were built in silico using the Institute for Genomic Research (TIGR) BAC end-sequence database (www.tigr.org/tdb/humgen/bac_end_search/bac_end_intro.html) and NIX analysis at the United Kingdom Human Genome Mapping Project (UK HGMP; www.hgmp.mrc.ac.uk/Registered/Webapp/nix). Sequence analysis of the BACs overlapping and near the breakpoints was performed with database tools and gene prediction software available in the NIX interface. The NCBI Map viewer (www.ncbi.nlm.nih.gov/mapview) was also used to study the genomic regions interrupted by the chromosomal breakpoints.

Embryo Collection

Human embryos were collected following British national guidelines [Polkinghorne, 1989] from terminated pregnancy material, with appropriate maternal written consent and approval from the Newcastle and North Tyneside National Health Service

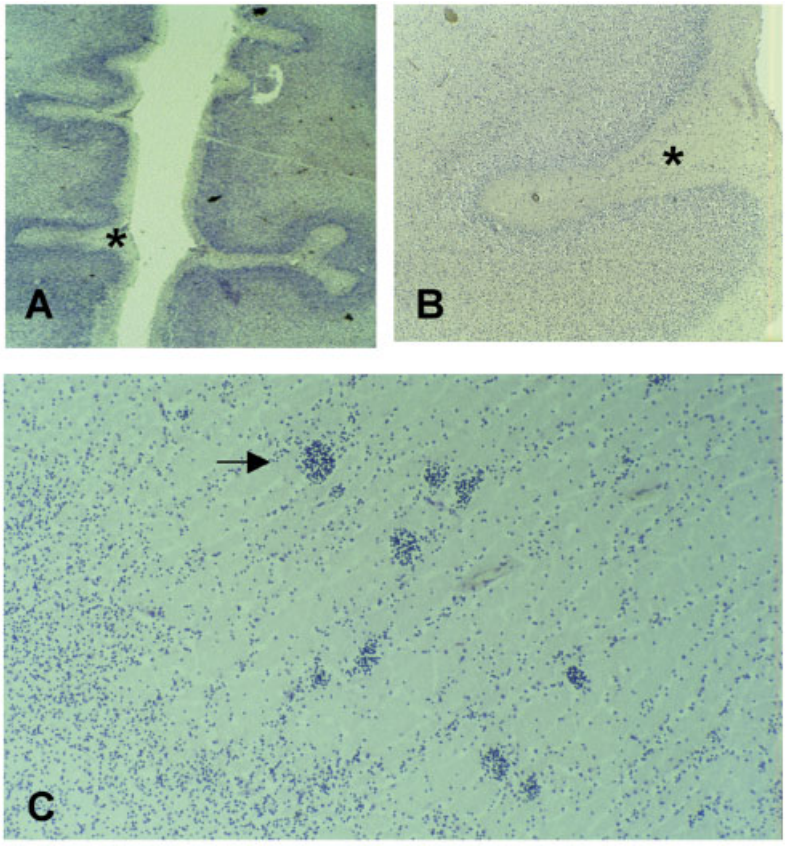

FIGURE 1. **Photomicrograph from the fetal polymicrogyric brain. A,B: Photomicrograph of polymicrogyric cortex shows multiple shallow sulci and fusion of the molecular layer inside gyri (asterisks). C: Photomicrograph of the white matter shows heterotopic neurons (arrow). [Color figure can be viewed in the online issue, which is available at www.interscience.wiley.com.]**

(NHS) Health Authority Joint Ethics Committee. The embryos were obtained from the Medical Research Council (MRC)–Wellcome Trust Human Developmental Biology Resource (HDBR; www.hdbr.org) at Newcastle. Embryos were collected into cold phosphate buffered saline (PBS), separated from surrounding tissue, and fixed overnight in 4% paraformaldehyde at 4°C, before short-term storage at 4°C in 70% ethanol. Placental tissue for karyotype analysis was sampled prior to fixation of the embryo tissue. The stage of development was assessed on the basis of external features according to the Carnegie staging protocol [O'Rahilly and Muller, 1987] modified for use with individual embryos rather than in comparisons of many embryos simultaneously [Bullen and Wilson, 1997; Bullen et al., 1998].

Tissue In Situ Hybridization

Digoxigenin-labeled sense and antisense probes to *NHEJ1* were generated by in vitro transcription of linearized plasmid DNA and purified through a ProbeQuant G-50 micro column (GE Healthcare). The probes were hybridized at 68°C using DIG Easy Hyb (Roche) following the method outlined in Franco et al. [2001] using an 8-minute proteinase K pretreatment to 8-μm tissue sections. Signal was detected by nitro blue tetrazolium/5-bromo-4-chloro-3-indolyl phosphate (NBT/BCIP) following posthybridization washes and incubation with an antidigoxygenin, alkaline phosphatase conjugated antibody.

RESULTS

Clinical Report

This female fetus came to medical attention at 27 weeks gestation when sonography demonstrated fetal hydrocephalus. A karyotype was performed on cultured amniocytes, and revealed a de novo apparently balanced translocation: 46,XX, t(2;7)(q36;p22). The pregnancy was terminated at 33 weeks based on these observations. At autopsy, growth parameters were normal for gestational age (weight 2,490 kg, height 46 cm, occipito-frontal circumference [OFC] 33 cm, foot 65 mm). External and visceral examination was normal except for the presence of a partial syndactyly of the fingers and complete syndactyly of toes two to four. Routine histology analysis showed no evidence of infection or inflammation. Examination of the brain confirmed the presence of hydrocephalus, and also demonstrated extensive PMG that appeared most severe in the occipital lobes and to a lesser extent the frontal lobes (Fig. 1A and B). Histological examination demonstrated a four-layered cortex comprised of a molecular layer, a layer of granular neurons, a poorly defined layer with few cells, and finally a layer of disorganized pyramidal neurons, as well as excess vascularization. The white matter demonstrated small groups of heterotopic neurons throughout with a prevalence in the white matter located beneath the polymicrogyric areas (Fig. 1C) as well as periventricular astrocytic gliosis. Cytomegalovirus serology was negative in the mother of this fetus.

Cytogenetic and Molecular Characterization of the Translocation

We first constructed a genomic contig with BAC clones covering the region likely to contain the breakpoints based on the karyotype observations (Fig. 2A). These clones were used as probes in FISH experiments on metaphase chromosome spreads from a lymphoblastoid cell line derived from the fetus. These serial hybridizations led to the identification of two clones spanning the translocation breakpoints: BAC RP11-803J6 in 2q35 and BAC RP11-1228A3 in 7p22 (Fig. 2B and C). The 2q35 breakpoint was more precisely mapped using Southern blot hybridizations. Serial hybridizations were performed with probes originating from the RP11-803J6 BAC clone until an aberrant restriction fragment was detected. Using one such probe a patient-specific restriction fragment was observed (Fig. 2D). This junction fragment was cloned and sequenced. Sequence analysis showed that it originates from 2q35 on one side and 7p22 on the other side. This data allowed us to amplify and sequence the translocation breakpoints on both derivative chromosomes and to show that the translocation is almost perfectly balanced (Fig. 2E). Indeed, comparison with wild-type sequences revealed an insertion of 11 bp on the

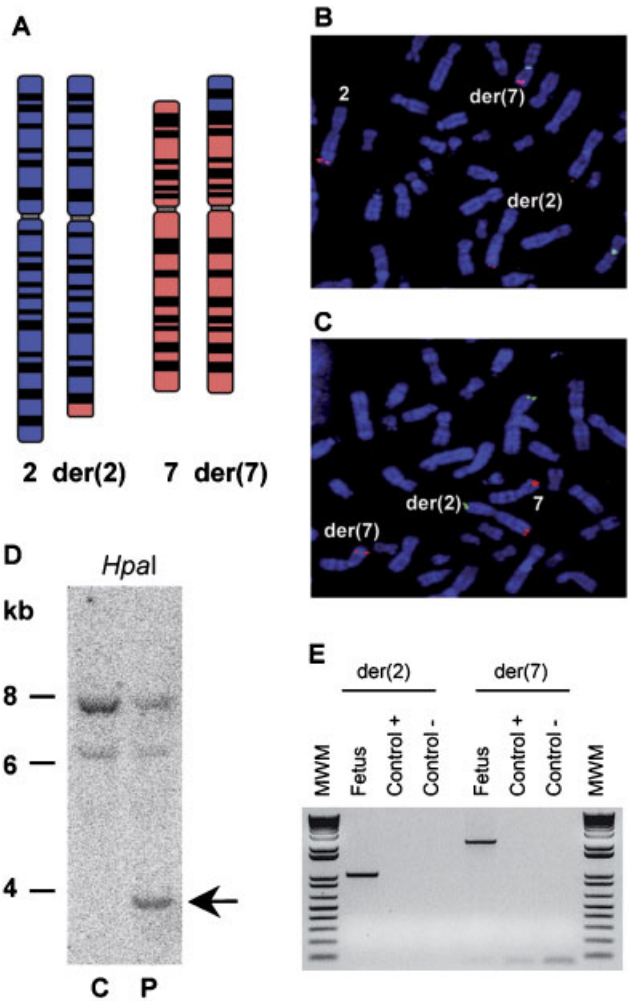

FIGURE 2. **Cytogenetic and molecular characterization of the breakpoints. A: Pictograms showing normal chromosomes 2 and 7 and their derivatives der(2) and der(7). B,C: Metaphase chromosomes of the fetus were used for FISH experiments with different clones spanning each breakpoint on der(2) and der(7): RP11-803J6 clone (signal in red) from chromosome 2 (B) and RP11-1228A3 clone (signal in red) from chromosome 7 (C). A centromeric BAC from chromosome 7 (signal in green) (B) and a telomeric BAC from short-arm of chromosome 2 (signal in green) (C) were used as control probes. D: Southern-blot hybridization of proband (P) and control (C) genomic DNA digested by *HpaI* with a probe corresponding to nucleotides 36989–37412 of clone RP11-803J6. E: PCR amplification of the two breakpoint-containing DNA fragments using the proband genomic DNA, a control DNA, or no DNA using primers originating from the two derivative chromosomes. Sequence of these amplicons allowed us to precisely localize the breakpoints.**

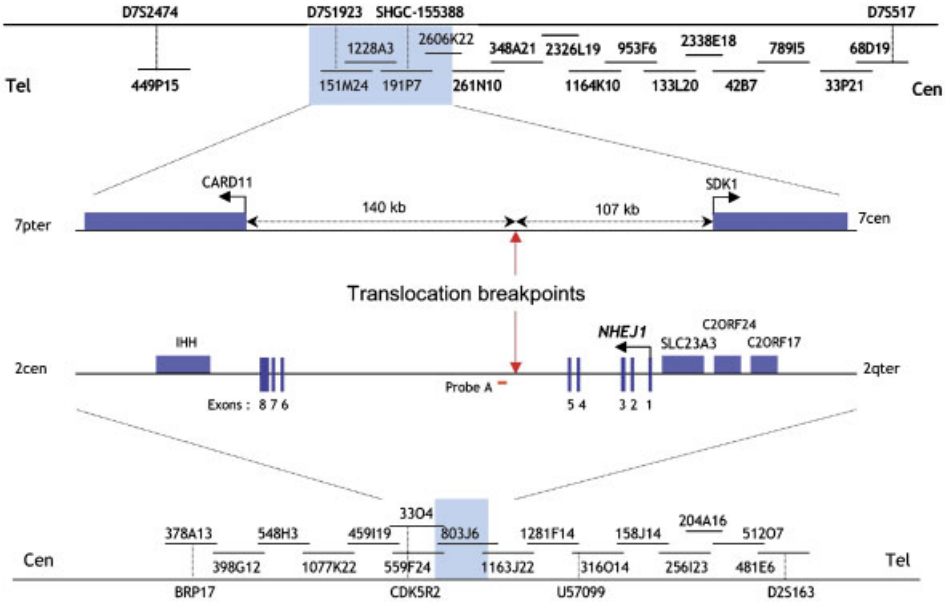

FIGURE 3. **Schematic representation of the breakpoint regions. Chromosome 7 (top) and chromosome 2 (bottom) BAC contigs showing the position of STSs in the critical region. In 7p22 the closest genes to the breakpoint are *CARD11* and *SDK1*. In 2q35, the breakpoint is located within intron 5 of *NHEJ1*. [Color figure can be viewed in the online issue, which is available at www.interscience.wiley.com.]**

derivative chromosome 2 and no insertion or deletion on the derivative chromosome 7 (data not shown). The 2q35 breakpoint is located at position 39387 in the sequence of clone RP11-803J6 and the 7p22 breakpoint at position 29861 in the sequence of clone RP11-191P7 (Fig. 3).

Sequence analysis using the NIX interface at HGMP indicates that the chromosome 7 breakpoint does not interrupt a known gene or anonymous expressed sequence tag (EST). The closest known genes are the CARD11 gene located 140 kb telomeric to the breakpoint and the *SDK1* gene located 107 kb centromeric to the breakpoint. A cluster of spliced ESTs (UniGene Hs.527001) is detected 35 kb telomeric to the breakpoint. We failed to detect a corresponding transcript using RT-PCR in different tissues including fetal brain (data not shown). *SDK1* is expressed in fetal brain and in several other tissues but it is not expressed in lymphoblastoid cell lines (Fig. 4A). *CARD11* is only weakly expressed in brain but is expressed in lymphoblastoid cell lines. We used a known SNP in the *CARD11* transcript for which the fetus was heterozygous and showed that the two *CARD11* alleles are expressed in the patient cell line in amounts similar to a control cell line (data not shown).

The 2q35 breakpoint interrupts the coding sequence of the *NHEJ1* gene. The breakpoint lies within intron 5 and interrupts the coding sequence for the NHEJ1 protein after amino acid 196 (Fig. 3). We tested the expression of the *SLC23A3* gene, a member of the solute carrier family, which is located 0.5 kb downstream of *NHEJ1*. This gene is expressed in kidney but not in fetal brain (Fig. 4A).

A Truncated NHEJ1 Transcript Is Present in the Patient's Cells

To determine the amount of *NHEJ1* transcripts present in the cells of the translocation patient, quantitative real-time PCR was performed with primers located before and after the translocation breakpoint and with primers spanning the translocation breakpoint (Fig. 5). The amount of *NHEJ1* transcript containing exons 6 to 8 (i.e., after the translocation breakpoint) is reduced by 50%. In contrast, the amount of transcript containing exons 1 to 5 is similar to the amount present in control cells. These results indicate that a truncated *NHEJ1* transcript is expressed in the patient cells.

Expression of NHEJ1 in Human and Mouse Tissues

Northern blots prepared using human mRNA originating from different brain regions were hybridized with a *NHEJ1* probe and revealed the presence of two transcripts (Fig. 4B). The stronger hybridizing band was estimated to be about 2.2 kb and the weaker band about 1.6 kb by comparison with RNA molecular weight markers. We searched the NCBI database for *NHEJ1* ESTs and identified EST sequences containing two different putative polyadenylation signals near a genuine poly(A) tail in the 3′ sequence. These putative sites are located in exon 8 and are separated by 600 bp, a size consistent with the size of the two transcripts. These observations were confirmed using 3′ rapid amplification of cDNA ends (RACE) and sequencing (data not shown).

RT-PCR experiments indicate that the *NHEJ1* transcripts are expressed in human fetal brain, lung, and kidney, with weaker signals detected in other tissues (Fig. 4A). Northern blot analysis using human nervous system tissues reveals that these transcripts are detected primarily in cerebellum and cerebral cortex (Fig. 4B). We also performed quantitative RT-PCR on total RNA from mouse embryos at different developmental stages. The *NHEJ1* transcript is highly expressed at embryonic day 12.5 (E12.5) with the level of expression decreasing thereafter, suggesting regulated expression during development (data not shown).

Expression of NHEJ1 During Early Human Development

The expression of *NHEJ1* during early human development was examined by in situ hybridization in tissue sections (Fig. 6). *NHEJ1* is expressed extensively in the central nervous system

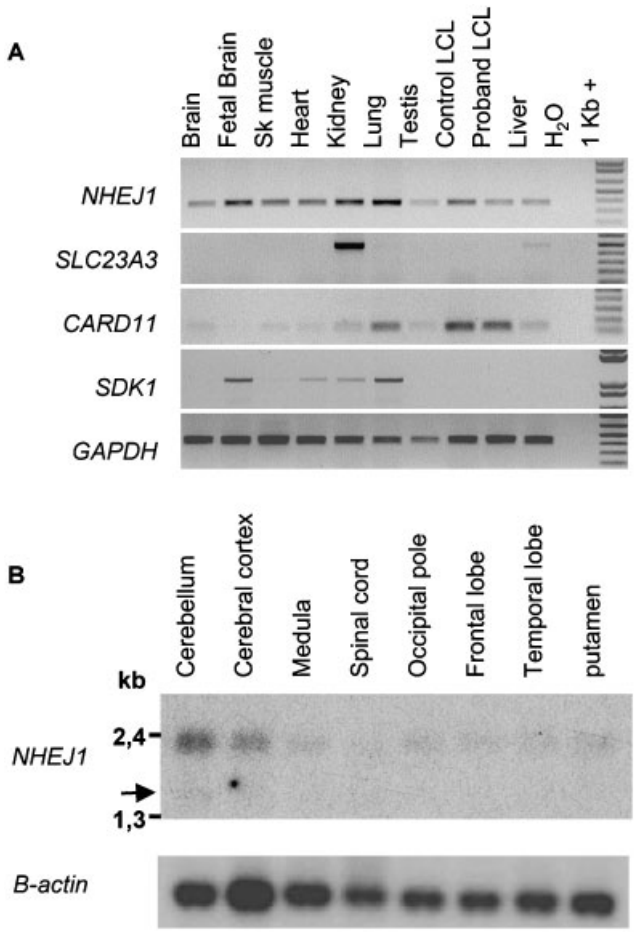

FIGURE 4. **Expression of the genes present in the breakpoint region. A: Expression pattern of the *NHEJ1*, *SLC23A3*, *CARD11*, and *SDK1* genes using tissue-specific RT-PCR. The glyceraldehyde-3-phosphate dehydrogenase (GAPDH) control is expressed in all tissues and was used as a control. B: Hybridization of a *NHEJ1* probe and a β-actin probe on a Northern blot prepared with RNA isolated from different regions of the adult human brain.**

(CNS) from the earliest stage examined (Carnegie stage 16 [CS16] at about 37 days of development; Fig. 6A). At later stages it is clear that expression is detected in the ventricular and subventricular zones, i.e., in neuroblasts rather than in differentiated neurons, and that there are regional differences in the levels of expression detected (Fig. 6B and C). In the lateral ventricles of the telencephalon, expression is relatively weak in the medial wall, and stronger laterally, including the future cerebral cortex. Signal is also detected in both lateral and medial ganglionic eminences (Fig. 6C). In the diencephalon, strong expression is detected in the dorsal thalamus and hypothalamus but expression is much weaker in the ventral thalamus (Fig. 6B). Expression is also strong in the developing cerebellum (Fig. 6B) but little or no expression is seen elsewhere in the developing hindbrain (Fig. 6A and C). *NHEJ1* is detected in alar midbrain (data not shown) and dorsal spinal cord (Fig. 6A and data not shown) and expression is also present in non-CNS tissues including the developing tongue, kidney, and digits (data not shown).

Mutation Screening in Patients With PMG

The fact that *NHEJ1* is highly expressed in the embryonic cerebral cortex and is disrupted in a fetus with PMG prompted us to screen additional patients affected by PMG for mutations in this gene. We therefore sequenced the coding region of *NHEJ1* in 72 patients with perisylvian PMG, which is the most common form, accounting for about 60% of patients [Leventer et al., 2001], and 13 patients with PMG and heterotopia. No disease-causing mutations were found. Other rare types of PMG that involve the anterior frontal or occipital lobes have not yet been tested.

DISCUSSION

We report investigations of a fetus with a malformation of cortical development consisting of extensive PMG and submicroscopic nodular neuronal heterotopia throughout the white matter that was found to have a de novo balanced translocation. One of the major issues with this type of study is to determine if the observed phenotype is a direct consequence of the presence of the chromosomal rearrangement. Balanced translocations occur at a frequency of one in 500 to 2000 live births and can also be identified in healthy individuals [Baptista et al., 2005, Warburton, 1991]. However, association of de novo balanced translocations and congenital abnormalities was estimated to be a two-fold [Warburton, 1991] to a six-fold increase [Bugge et al., 2000] compared to the general population. This observation suggests that a causative link exists in many cases between the interruption or modulation of gene expression by a balanced rearrangement and the phenotype of its carrier.

To better understand the relationship between genotype and phenotype in the patient that we studied, we mapped, cloned and sequenced the two translocation breakpoints. We found that the translocation is molecularly balanced with no significant loss or gain of DNA. This is the most favorable situation, with a simple exchange of genetic material between two chromosomes. More interestingly, we showed that the *NHEJ1* gene, also called *Cernunnos*, *XLF*, or *FJL12610* in two recent reports [Ahnesorg et al., 2006; Buck et al., 2006], is the single transcription unit disrupted by the translocation breakpoint in the cells of the patient. Obviously, this finding makes it the best candidate to be involved in the phenotype. Nonetheless, it was important to consider the genomic context in the vicinity of the breakpoints and to question the putative implication of the other genes located in this area. On chromosome 7, the genes located the most closely to the breakpoint are *SDK1* and *CARD11*. *SDK1* was shown to be involved in synaptic adhesion during the development of the retina [Yamagata et al., 2002] and in the pathogenesis of HIV-associated nephropathy [Kaufman et al., 2004]. We cannot rule out the possibility that this gene is implicated in the phenotype. However, given its genomic location 100 kb distal to the breakpoint and its putative function, its involvement in the phenotype of our patient is unlikely. We could not test if the transcription of this gene was altered in the patient cells because *SDK1* is not expressed in lymphoblastoid cell lines. *CARD11* has been classified as a member of the membrane-associated guanylate kinase (MAGUK) proteins with a caspase recruitment domain. It was shown to be involved in the immune response with an implication in NF-KappaB signaling [Bertin et al., 2001]. We have shown that the two alleles of this gene are expressed in the patient lymphoblastoid cell line, ruling out a major positional effect, at least in this cell type. On chromosome 2, *IHH* (Indian Hedgehog) is the best-characterized gene near the breakpoint. Mice deficient for *Ihh* have abnormal skeletal morphogenesis [St-Jacques et al., 1999]. Mutations in the human *IHH* gene result in brachydactyly type A1 (MIM# 112500) and acrocapitofemoral dysplasia (MIM# 607778). Also located on chromosome 2 is the human *SLC23A3* gene, which was not previously characterized other than

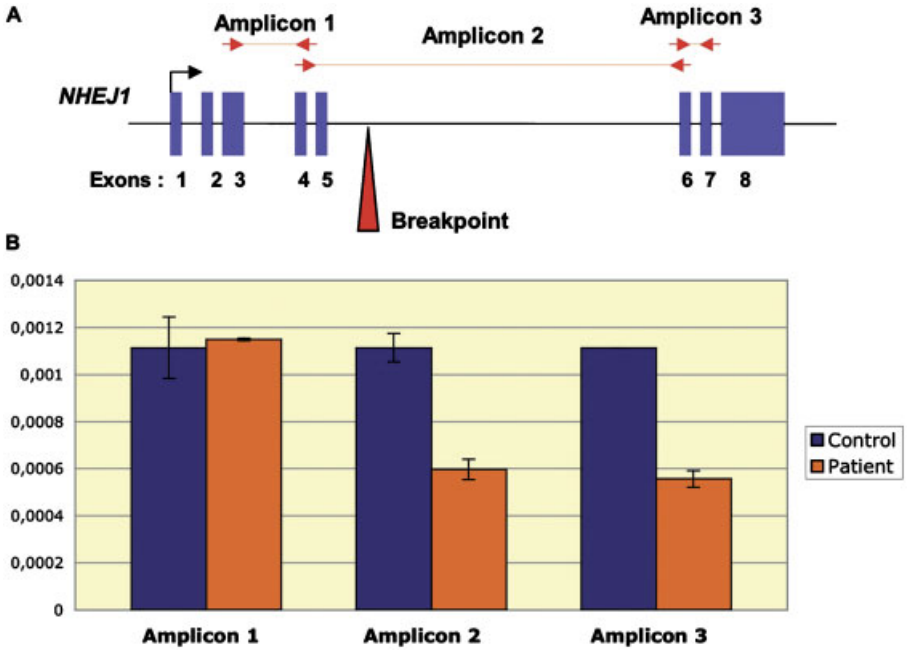

FIGURE 5. **A truncated *NHEJ1* transcript is present in the patient cells. A:** Schematic representation of the *NHEJ1* gene showing the position of the primers used for the quantitative PCR. Amplicon 2 overlaps the breakpoint and amplifies only the normal allele while amplicons 1 and 3 can amplify putative 5′ or 3′ portions of the disrupted allele in the patient lymphocytes. **B:** Quantitative real-time RT-PCR showing the relative expression of the different portions of NHEJ1 compared to β-actin in control and patient cells. The expression levels of amplicons 2 and 3 were normalized and set at the same value than amplicon 1 to allow direct comparisons. [Color figure can be viewed in the online issue, which is available at www.interscience.wiley.com.]

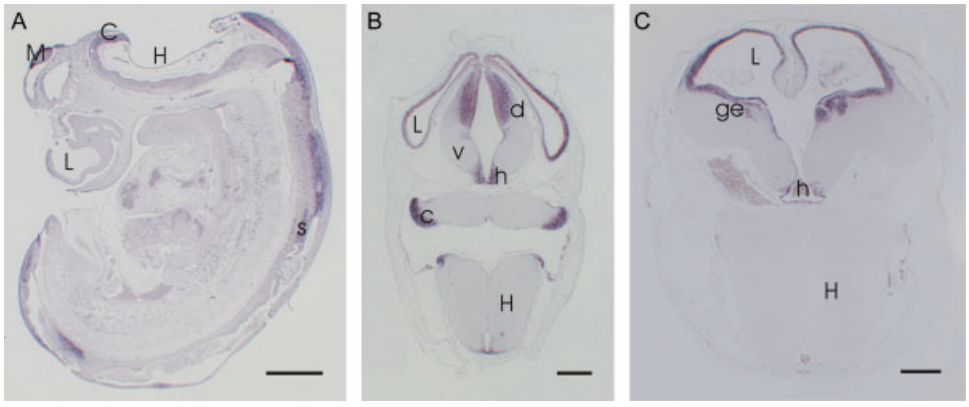

FIGURE 6. **Expression of NHEJ1 during early human development. A:** Parasagittal section of CS16 embryo (~37 days of development) showing expression in the dorsal midbrain, hindbrain (developing cerebellum) and spinal cord. **B:** Transverse section of CS21 embryo (~52 days of development) showing expression in the lateral ventricle, dorsal thalamus, ventral thalamus (weakly), and hypothalamus in the developing forebrain and the cerebellum in the developing hindbrain. **C:** Transverse section of CS23 embryo (~56 days of development) showing expression in the lateral ventricles and ganglionic eminences of the developing forebrain. The expression patterns were confirmed in two embryos at stages CS16, CS20, and CS21, and one embryo at CS23. Tissue in situ hybridization was carried out as described in Materials and Methods using an *NHEJ1* antisense probe. Corresponding sections were hybridized to an *NHEJ1* sense probe and no signal was detected (data not shown). In parts A, B, and C, the signal is detected as a blue-purple deposit. c, cerebellum; d, dorsal thalamus; ge, ganglionic eminence; h, hypothalamus; H, hindbrain; L, lateral ventricle; M, midbrain; v, ventral thalamus.

its ability to encode a member of the large family of solute carrier proteins. None of these genes appears to be an obvious candidate for a neuronal migration disorder.

To further address the question of whether *NHEJ1* was involved in the phenotype of our patient, it was important to determine its expression pattern since this has not been described before. Of particular interest was the study of its expression during early development of the human brain. We found that the expression pattern of *NHEJ1* is in good agreement with our hypothesis that it could play a role in brain development. Indeed, we showed that during early human development, the *NHEJ1* transcript is detected preferentially in the CNS including in regions that subsequently give rise to the cerebral cortex. In the adult human brain, the transcript is also abundant in the cerebral cortex and in the cerebellum. More specifically, *NHEJ1* is preferentially expressed in the neocortical ventricular and subventricular zones

during periods of extensive neurogenesis. In contrast, there is little or no expression in the cortical plate or intermediate zone. This expression pattern suggests an expression in progenitor cells rather than in postmitotic neurons and it is in good agreement with the phenotype observed in the translocation patient consisting mainly of a neurological phenotype. It is a similar pattern to that observed for *GPR56*, a gene whose mutations cause frontoparietal bilateral PMG, which is also highly expressed in neuronal progenitors [Piao et al., 2004]. Since the proper cortical size and shape is determined by the rate of production of neurons and glial cells in proliferative zones [reviewed in Haydar et al., 1999] it is possible that an early change in the expression of a gene strongly expressed in neuronal precursors could alter subsequent patterning of the cerebral cortex. Of the other sites of expression, both in CNS and non-CNS tissues, the only one that appears directly relevant to the phenotype is in the developing digits. The patient had syndactyly of the fingers and toes. Considering this aspect of the phenotype, the screening of NHEJ1 in patients with polymicrogyria associated with limb defects deserves to be considered in the future.

Interestingly, the disruption of the coding region of *NHEJ1* does not lead to a simple reduction of its expression by 50%. The portion of the transcript located 3′ to the breakpoint (exons 6 to 8) on the translocated chromosome is no longer detectable in the patient's cells. In contrast, the 5′ region of the transcript located upstream of the breakpoint (exons 1 to 5) is expressed in similar amounts to the wild-type allele. This suggests that a truncated transcript (possibly also containing a chromosome 7 transcribed DNA fragment) is produced and is stable in the patient's cells. This truncated transcript encodes the NH2-terminal portion of NHEJ1 containing the first 196 amino acids.

The recently described *NHEJ1* mutations cause a phenotype that differs significantly from the phenotype of our translocation patient. In addition, the immunodeficiency and microcephaly syndrome is autosomal recessive, whereas our patient has a wild-type copy of the gene. If the disruption of *NHEJ1* is responsible for the observed phenotype, one explanation could be that the expression of the truncated transcript causes a dominant negative effect. The mutations identified in immunodeficient and microcephalic patients are of various types with both missense and nonsense mutations [Ahnesorg et al., 2006; Buck et al., 2006]. However, nonsense-mediated mRNA decay was not tested and it is not known if these patients express an abnormal transcript or no transcript at all. Indeed, one of the reported early truncating mutations leads to a complete absence of NHEJ1 protein and an unstable transcript [Ahnesorg et al., 2006]. This point is very important since one may wonder whether or not the heterozygous parents of the affected individuals are expressing an abnormal but stable transcript from their mutated allele. If not, one of the reasons why the translocation patient presents a different phenotype could be the presence of a significant amount of truncated NHEJ1 protein, especially because NHEJ1 is able to homo- or heterodimerize. Truncated NHEJ1 proteins may be able to sequester interactors such as XRCC4 into inactive dimers.

Whatever mechanism is true, it would be interesting to investigate the functionality of the NHEJ pathway in the cells of our patient or to perform MRI investigations in the immunodeficient patients carrying truncating mutations to determine if they do not suffer from subtle cortical disorganization.

ACKNOWLEDGMENTS

We thank Regina Betz, Renzo Guerrini, and Daniela Pilz for sending samples of patients. We thank Mareike Schnaars for her help during the initial phases of this work. The human embryonic tissue was provided by the Joint Medical Research Council (MRC)-Wellcome Human Developmental Biology Resource at Institute of Human Genetics (IHG), Newcastle upon Tyne (www.hdbr.org). V.C. is the recipient of a Ministère de la Recherche et de la Technologie (MRT) fellowship.

REFERENCES

Ahnesorg P, Smith P, Jackson SP. 2006. XLF interacts with the XRCC4-DNA ligase IV complex to promote DNA nonhomologous end-joining. Cell 124:301–313.

Aligianis IA, Johnson CA, Gissen P, Chen D, Hampshire D, Hoffmann K, Maina EN, Morgan NV, Tee L, Morton J, Ainsworth JR, Horn D, Rosser E, Cole TR, Stolte-Dijkstra I, Fieggen K, Clayton-Smith J, Megarbane A, Shield JP, Newbury-Ecob R, Dobyns WB, Graham JM, Jr, Kjaer KW, Warburg M, Bond J, Trembath RC, Harris LW, Takai Y, Mundlos S, Tannahill D, Woods CG, Maher ER. 2005. Mutations of the catalytic subunit of RAB3GAP cause Warburg Micro syndrome. Nat Genet 37: 221–223.

Baptista J, Prigmore E, Gribble SM, Jacobs PA, Carter NP, Crolla JA. 2005. Molecular cytogenetic analyses of breakpoints in apparently balanced reciprocal translocations carried by phenotypically normal individuals. Eur J Hum Genet 13:1205–1212.

Barkovich AJ, Lindan CE. 1994. Congenital cytomegalovirus infection of the brain: imaging analysis and embryologic considerations. Am J Neuroradiol 15:703–715.

Barth PG. 1992. Migrational disorders of the brain. Curr Opin Neurol Neurosurg 5:339–343.

Bertin J, Wang L, Guo Y, Jacobson MD, Poyet JL, Srinivasula SM, Merriam S, DiStefano PS, Alnemri ES. 2001. CARD11 and CARD14 are novel caspase recruitment domain (CARD)/membrane-associated guanylate kinase (MAGUK) family members that interact with BCL10 and activate NF-kappa B. J Biol Chem 276:11877–11882.

Brooks AS, Bertoli-Avella AM, Burzynski GM, Breedveld GJ, Osinga J, Boven LG, Hurst JA, Mancini GM, Lequin MH, de Coo RF, Matera I, de Graaff E, Meijers C, Willems PJ, Tibboel D, Oostra BA, Hofstra RM. 2005. Homozygous nonsense mutations in KIAA1279 are associated with malformations of the central and enteric nervous systems. Am J Hum Genet 77:120–126.

Buck D, Malivert L, de Chasseval R, Barraud A, Fondaneche MC, Sanal O, Plebani A, Stephan JL, Hufnagel M, le Deist F, Fischer A, Durandy A, de Villartay JP, Revy P. 2006. Cernunnos, a novel nonhomologous end-joining factor, is mutated in human immunodeficiency with microcephaly. Cell 124:287–299.

Bugge M, Bruun-Petersen G, Brondum-Nielsen K, Friedrich U, Hansen J, Jensen G, Jensen PK, Kristoffersson U, Lundsteen C, Niebuhr E, Rasmussen KR, Rasmussen K, Tommerup N. 2000. Disease associated balanced chromosome rearrangements: a resource for large scale genotype-phenotype delineation in man. J Med Genet 37:858–865.

Bullen P, Wilson D. 1997. The Carnegie staging of human embryos: a practical guide. In: Strachan T, Lindsay S, Wilson DI, editors. Molecular genetics of early human development. Oxford UK: Bios Scientific Publishers. p 27–35.

Bullen PJ, Robson SC, Strachan T. 1998. Human post-implantation embryo collection: medical and surgical techniques. Early Hum Dev 51: 213–221.

Callebaut I, Malivert L, Fischer A, Mornon JP, Revy P, de Villartay JP. 2006. Cernunnos interacts with the XRCC4-DNA-ligase IV complex and is homologous to the yeast nonhomologous end-joining factor Nej1. J Biol Chem 281:13857–13860.

Chang BS, Piao X, Bodell A, Basel-Vanagaite L, Straussberg R, Dobyns WB, Qasrawi B, Winter RM, Innes AM, Voit T, Grant PE, Barkovich AJ, Walsh CA. 2003. Bilateral frontoparietal polymicrogyria: clinical and radiological features in 10 families with linkage to chromosome 16. Ann Neurol 53:596–606.

Chong SS, Pack SD, Roschke AV, Tanigami A, Carrozzo R, Smith AC, Dobyns WB, Ledbetter DH. 1997. A revision of the lissencephaly

and Miller-Dieker syndrome critical regions in chromosome 17p13.3. Hum Mol Genet 6:147–155.

Dobyns WB, Pagon RA, Armstrong D, Curry CJR, Greenberg F, Grix A, Holmes LB, Laxova R, Michels VV, Robinow M, Zimmerman RL. 1989. Diagnostic criteria for Walker-Warburg syndrome. Am J Med Genet 32: 195–210.

Evrard P, Caviness VS, Prats-Vinas J, Lyon G. 1978. The mechanism of arrest of neuronal migration in the Zellweger malformation: an hypothesis based upon cytoarchitectonic analysis. Acta Neuropathol 41: 109–117.

Fox JW, Lamperti ED, Eksioglu YZ, Hong SE, Feng Y, Graham DA, Scheffer IE, Dobyns WB, Hirsch BA, Radtke RA, Berkovic SF, Huttenlocher PR, Walsh CA. 1998. Mutations in filamin 1 prevent migration of cerebral cortical neurons in human periventricular heterotopia. Neuron 21:1315–1325.

Franco D, de Boer PA, de Gier-de Vries C, Lamers WH, Moorman AF. 2001. Methods on in situ hybridization, immunohistochemistry and beta-galactosidase reporter gene detection. Eur J Morphol 39: 169–191.

Glaser T, Jepeal L, Edwards JG, Young SR, Favor J, Maas RL. 1994. PAX6 gene dosage effect in a family with congenital cataracts, aniridia, anophthalmia and central nervous system defects. Nat Genet 7: 463–471.

Gleeson JG, Allen KM, Fox JW, Lamperti ED, Berkovic S, Scheffer I, Cooper EC, Dobyns WB, Minnerath SR, Ross ME, Walsh CA. 1998. *doublecortin*, a brain-specific gene mutated in human X-linked lissencephaly and double cortex syndrome, encodes a putative signaling protein. Cell 92:63–72.

Guerrini R, Sicca F, Parmeggiani L. 2003. Epilepsy and malformations of the cerebral cortex. Epileptic Disord 5:S9–S26.

Haltia M, Leivo I, Somer H, Pihko H, Paetau A, Kivela T, Tarkkanen A, Tome F, Engvall E, Santavuori P. 1997. Muscle-eye-brain disease: a neuropathological study. Ann Neurol 41:173–180.

Haydar TF, Kuan CY, Flavell RA, Rakic P. 1999. The role of cell death in regulating the size and shape of the mammalian forebrain. Cereb Cortex 9:621–626.

Iannetti P, Nigro G, Spalice A, Faiella A, Boncinelli E. 1998. Cytomegalovirus infection and schizencephaly: case reports. Ann Neurol 43:123–127.

Jansen A, Andermann E. 2005. Genetics of polymicrogyria syndromes. J Med Genet 42:369–378.

Kaufman L, Hayashi K, Ross MJ, Ross MD, Klotman PE. 2004. Sidekick-1 is upregulated in glomeruli in HIV-associated nephropathy. J Am Soc Nephrol 15:1721–1730.

Kelley RI, Datta NS, Dobyns WB, Hajra AK, Moser AB, Noetzel MJ, Zackai EH, Moser HW. 1986. Neonatal adrenoleukodystrophy: new cases, biochemical studies, and differentiation from Zellweger and related peroxisomal polydystrophy syndromes. Am J Med Genet 23: 869–901.

Kuzniecky R, Jackson G. 1995. Magnetic resonance in epilepsy. New York: Raven Press. p 197–221.

Leventer RJ, Lese CM, Cardoso C, Roseberry J, Weiss A, Stoodley N, Pilz DT, Villard L, Nguyen K, Clark GD, Shaffer LG, Guerrini R, Dobyns WB. 2001. A study of 220 patients with polymicrogyria delineates distinct phenotypes and reveals genetic loci on chromosomes 1p, 2p, 6q, 21q and 22q. Am J Hum Genet 69S4:177.

Lo Nigro C, Chong CS, Smith AC, Dobyns WB, Carrozzo R, Ledbetter DH. 1997. Point mutations and an intragenic deletion in LIS1, the lissencephaly causative gene in isolated lissencephaly sequence and Miller-Dieker syndrome. Hum Mol Genet 6:157–164.

Meencke H-J, Veith G. 1992. Migration disturbances in epilepsy. In: Engel JJ, Wasterlain C, Cavalhero EA, Heinemann U, Avanzini G, editors. Molecular neurobiology of epilepsy. New York: Elsevier Science Publishers. p 31–40.

Mitchell TN, Free SL, Williamson KA, Stevens JM, Churchill AJ, Hanson IM, Shorvon SD, Moore AT, van Heyningen V, Sisodiya SM. 2003. Polymicrogyria and absence of pineal gland due to PAX6 mutation. Ann Neurol 53:658–663.

O'Rahilly R, Muller F. 1987. Developmental stages in human embryos. Carnegie Institute, Washington, Publication no. 637.

Piao X, Hill RS, Bodell A, Chang BS, Basel-Vanagaite L, Straussberg R, Dobyns WB, Qasrawi B, Winter RM, Innes AM, Voit T, Ross ME, Michaud JL, Descarie JC, Barkovich AJ, Walsh CA. 2004. G protein-coupled receptor-dependent development of human frontal cortex. Science 303:2033–2036.

Piao X, Chang BS, Bodell A, Woods K, Benzeev B, Topcu M, Guerrini R, Goldberg-Stern H, Sztriha L, Dobyns WB, Barkovich AJ, Walsh CA. 2005. Genotype-phenotype analysis of human frontoparietal polymicrogyria syndromes. Ann Neurol 58:680–687.

Polkinghorne J. 1989. Guidelines on the research use of foetuses and foetal material. London, HMSO, CM762.

Robin NH, Taylor CJ, McDonald-McGinn DM, Zackai E, Bingham P, Collins KJ, Earl D, Gill D, Granata T, Guerrini R, Katz N, Kimonis V, Leventer RJ, Lin J-P, Lynch DR, Mohammed SN, Massey RF, McDonald M, Rogers CR, Splitt M, Stevens CA, Tischkowitz MD, Stoodley N, Pilz DT, Dobyns WB. 2006. Polymicrogyria and deletion 22q11.2 syndrome: window to the etiology of a common cortical malformation. Am J Med Genet A 140:2416–2425.

Sprecher E, Ishida-Yamamoto A, Mizrahi-Koren M, Rapaport D, Goldsher D, Indelman M, Topaz O, Chefetz I, Keren H, O'Brien T J, Bercovich D, Shalev S, Geiger D, Bergman R, Horowitz M, Mandel H. 2005. A mutation in SNAP29, coding for a SNARE protein involved in intracellular trafficking, causes a novel neurocutaneous syndrome characterized by cerebral dysgenesis, neuropathy, ichthyosis, and palmoplantar keratoderma. Am J Hum Genet 77:242–251.

St-Jacques B, Hammerschmidt M, McMahon AP. 1999. Indian hedgehog signaling regulates proliferation and differentiation of chondrocytes and is essential for bone formation. Genes Dev 13:2072–2086.

Takada K, Nakamura H, Takashima S. 1988. Cortical dysplasia in Fukuyama congenital muscular dystrophy (FCMD): a Golgi and angioarchitectonic analysis. Acta Neuropathol 76:170–178.

Villard L, Nguyen K, Cardoso C, Martin CL, Weiss AM, Sifry-Platt M, Grix AW, Graham JM Jr, Winter RM, Leventer RJ, Dobyns WB. 2002. A locus for bilateral perisylvian polymicrogyria maps to Xq28. Am J Hum Genet 70:1003–1008.

Vinters HV, Fisher RS, Cornford ME, Mah V, Lenard Secor D, DeRosa MJ, Comair YG, Peacock WJ, Shields WD. 1992. Morphological substrates of infantile spasms: studies based on surgically resected cerebral tissue. Childs Nerv Syst 8:8–17.

Warburton D. 1991. De novo balanced chromosome rearrangements and extra marker chromosomes identified at prenatal diagnosis: clinical significance and distribution of breakpoints. Am J Hum Genet 49: 995–1013.

Yamagata M, Weiner JA, Sanes JR. 2002. Sidekicks: synaptic adhesion molecules that promote lamina-specific connectivity in the retina. Cell 110:649–660.